Proceedings of the Canadian Society for Mechanical Engineering International Congress
32nd Annual Conference of the Computational Fluid Dynamics Society of Canada
Canadian Society of Rheology Symposium
CSME/CFDSC/CSR 2025
May 25–28, 2025, Montréal, Québec, Canada

EXPERIMENTAL REPEATABILITY ASSESSMENT OF A METROLOGY ASSISTED ROBOTIC ASSEMBLY SYSTEM USING IGPS TRACKING

William Babin[1], Ahmed Joubair[1], Souheil-Antoine Tahan[2]

[1]Department of Automated Manufacturing Engineering, École de technologie Supérieure, Montréal, Canada
[2]Department of Mechanical Engineering, École de technologie Supérieure, Montréal, Canada

2025-01-31

***Abstract*—**Large-scale metrology tools like indoor GPS (iGPS) are increasingly used in robotic assembly for large and complex parts due to their accuracy over extensive workspaces. iGPS is particularly suitable for jigless assembly, where high accuracy and repeatability are required without the need for traditional fixtures. However, integrating iGPS into Measurement-Assisted Assembly (MAA) systems raises uncertainties regarding repeatability, which is critical for industrial applications. This empirical study evaluates the repeatability of a robotic MAA system using iGPS as an external encoder. The experimental setup includes a six-axis robotic arm, a pre-measured artifact simulating an assembly part, and an iGPS system for position and orientation feedback. Positional repeatability was assessed under controlled conditions inspired by the ISO 9283 standard. Results showed a spatial mean positional repeatability of 31 μm during static mounting and 26 μm when the artifact was removed between each measurement (both with 99.73% confidence). These results validate the potential of a robot augmented with iGPS tracking as a robust system for guiding jigless assembly. The developed framework can be used in the future to better understand accuracy and repeatability of iGPS-augmented robotic systems.

***Keywords-component*—iGPS; Metrology; Jigless Assembly; Measurement Assisted Assembly**

I. INTRODUCTION

Large-Scale Metrology (LSM) tools, such as laser trackers, photogrammetry systems, and indoor GPS (iGPS) systems, play a critical role in many manufacturing processes, particularly in industries like aerospace and automotive, where medium- and large-scale components demand high accuracy. Among these systems, iGPS stands out due to its decentralized nature and large usable workspace. The integration of iGPS systems with robotic manipulation in the context of Measurement-Assisted Assembly (MAA) is particularly promising, as these systems enable jigless assembly, eliminating the need for traditional fixtures. This approach improves flexibility and reduces manufacturing costs, especially in areas where traditional part interchangeability has not yet been fully realized. However, despite its advantages, integrating iGPS into robotic systems for MAA presents challenges. Notably, the repeatability error of these systems is not well established, posing a significant barrier to their adoption in industrial applications. This study aims to evaluate the repeatability capabilities of a robotic MAA system using iGPS as an external encoder. The experimental setup comprises a six-axis robotic arm, a pre-measured artifact simulating an assembly part, and an iGPS system providing position and orientation feedback. The artifact was first measured using a coordinate measuring machine (CMM) to establish a reference for its key characteristics relative to the robot's attachment point. The robot then performed multiple placement trials under controlled conditions inspired by ISO 9283 guidelines. Deviations in the artifact's position and orientation were tracked using the iGPS system. To mitigate thermal effects on the results, the optimal warm-up time under load conditions was determined beforehand. The analysis focused on quantifying positional and orientation repeatability, which directly translates to the system's capacity to consistently position a key feature in space. In this case, the artifact's key characteristic is an adjacent surface. Engineering assembly requirements often necessitate the precise placement of key features within specified tolerances (e.g., Euclidean distance, gap, true position, etc.). Thus, process capabilities must be studied to link engineering requirements with system performance.This paper is structured as follows: Chapter I presents the background and related work, while Chapters II and III describe the experimental setup and methodology. Chapter IV presents the main results, and finally, Chapter V discusses conclusions and future research

directions.

II. BACKGROUND AND RELATED WORK

A. The iGPS System

The iGPS is an angle-based large-scale metrology positioning system. Transmitters are positioned within the work area, each rotating at a unique frequency between 40 Hz and 50 Hz. Each transmitter emits two infrared laser beam planes at a tilt along with a pulsed timing signal. The receivers convert these laser signals into voltage, which is then wirelessly transmitted to a computer system that computes the receiver's position. Several articles discuss the working principles of iGPS systems, such as [1] and [2]. A minimum of two transmitters is required to calculate the receiver's position, while using four transmitters significantly improves accuracy [3]. iGPS systems offer a significant advantage over other LSM instruments, primarily due to their decentralized nature. Receivers do not require a connection to a centralized unit. The iGPS transmitters can be placed directly in production environments, and a large number of receivers can be used simultaneously. The range covered by each emitter extends from 2 to 55 m, making these systems particularly useful in large-part assembly contexts [4]. The accuracy of these systems is largely configuration-dependent. The workspace size, number of transmitters, and system calibration all influence measurement accuracy [5]. Environmental conditions such as temperature, humidity, vibrations, luminosity, and reflectiveness of nearby surfaces also affect accuracy. For an eight-transmitter configuration in a 10 m × 20 m area, the manufacturer claims a 0.150 mm 3D point uncertainty, a 0.250 mm dynamic 3D point uncertainty for sensor velocities below 0.5 m/s, and a 0.90 mrad angular uncertainty, all of which are given with 95% confidence intervals [6].

B. The use of iGPS for Measurment Assisted Assembly

The feasibility of using iGPS systems as external encoders for robotic assembly tasks has been proven and demonstrated in [7] and [8]. Research has also validated the use of iGPS systems as external measurement devices for robot control, as shown in [5]. The predicted accuracy of robots using iGPS as external encoders is within 0.3 mm [5]. Studies on improving the dynamic tracking capabilities of iGPS have also been conducted [9]. Additionally, iGPS systems have been used to enhance serial robot accuracy through real-time dynamic compensation methods, as shown in [10]. Finally, an experimental setup was employed to evaluate the performance of iGPS systems in an MAA process, as shown in [11]. The resulting iGPS repeatability was within the 0.01 mm to 0.16 mm range for a manually controlled assembly process [11].

C. Gap in the Existing Research

To the best of our knowledge, no comprehensive study has been conducted to evaluate the repeatability of a system composed of a robotic arm and an iGPS system as an external encoder. Second, no connection has been established between the repeatability of such systems and how it translates to assembly engineering requirements. Extracting the confidence intervals (e.g., $\pm 3\sigma$) for key feature placements from the evaluated repeatability can directly link process capabilities to the engineering requirements of the product being assembled, which could facilitate the adoption of these systems.

D. Overview of ISO 9283

The ISO 9283 guidelines provide a standardized method for evaluating the repeatability and accuracy of serial robots. This standard defines key parameters, including test positions, the number of cycles, load and speed conditions, test trajectories, and environmental factors. For repeatability testing of a 6-axis serial manipulator, the test positions used to assess repeatability and accuracy define a plane within a cube, as shown in Fig. 1.

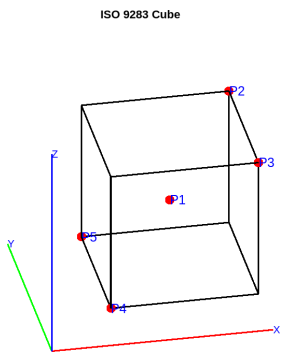

Figure. 1. ISO 9283 points used for repeatability testing of a 6 axis robot.

The recommended trajectory is P1-P2-P3-P4-P5, executed for n=30 cycles, with data collected at each point. Pose repeatability, as defined in ISO 9283, is the radius of a sphere centered at the barycenter of the gathered data points for the same commanded pose, as shown in (1). RP_l is the resulting radius, $\bar{l}$ the barycenter of the sphere, and σ_l the standard deviation.

$$RP_l = \bar{l} + 3\sigma_l \tag{1}$$

$$\bar{l} = \frac{1}{n}\sum_{j=i}^{n} l_j \tag{2}$$

$$l_j = \sqrt{(x_j - \bar{x})^2 + (y_j - \bar{y})^2 + (z_j - \bar{z})^2} \tag{3}$$

The ISO 9283 guidelines also define orientation repeatability as $\pm 3\sigma$ (99.73%), as shown in equation (2). The angles α, β, and γ represent roll, pitch, and yaw, respectively.

$$RP_\alpha = \pm 3\sigma_\alpha \tag{4}$$

$$RP_\beta = \pm 3\sigma_\beta \tag{5}$$

$$RP_\gamma = \pm 3\sigma_\gamma \tag{6}$$

To conduct such repeatability tests, ISO 9283 recommends performing a robot warm-up cycle beforehand. Thermal drift is an important factor in robot accuracy and repeatability. However, no specific warm-up time is defined, as it is largely influenced by the load conditions and the specific test environment. It was shown in [12] that a robot's joint temperatures reach a stable state after a certain amount of time under load conditions. This steady state must be achieved before conducting repeatability tests to mitigate thermal expansion effects. Finally, the robot used in this experimental study is the IRB120™. Its uncalibrated repeatability and accuracy were evaluated in [13].

III. Methodology

A. The Experimental Setup

The experimental setup consists of an artifact specifically machined to interface directly with the flange of the IRB120™ robot. Three tooling nests, each equipped with magnets, were installed on the artifact to accommodate the i5IS receivers. These tooling nests are offset relative to the center of the cube, ensuring that the resulting center of mass is closer to the robot attachment point. Euclidean distances between the centers of the tooling nests and their coordinates relative to the flange interface were measured with a CMM, allowing the transformation matrix between the robot flange and the artifact to be determined. The artifact is shown in Fig. 2.

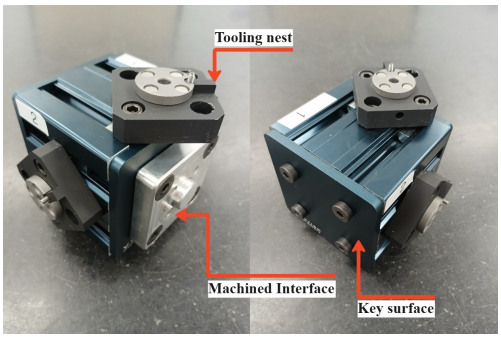

Figure. 2. The designed artifact.

For all tests conducted, the robot was mounted on a steel plate placed on a granite table. The corner of the granite table was used as a reference to define the iGPS using the i6 probe. The experimental setup is shown in Fig. 3.

B. Tests procedures

1) Ideal warm-up time: To determine the ideal warm-up time, temperature measurements were recorded every 5 minutes during operation at four different locations on the robot arm's surface using an infrared thermometer. The four locations are shown in Fig. 4. First, a control test was conducted with an arbitrary linear movement between two points at high speed (100 mm/s). Then, the same test was repeated for the same load, speed (10 mm/s), and commanded points used in other test procedures.

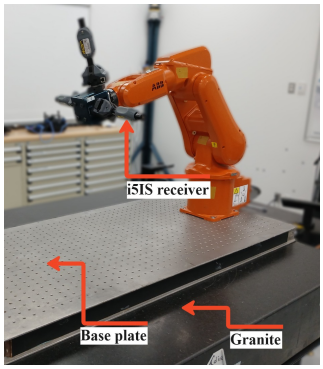

Figure. 3. The experimental setup.

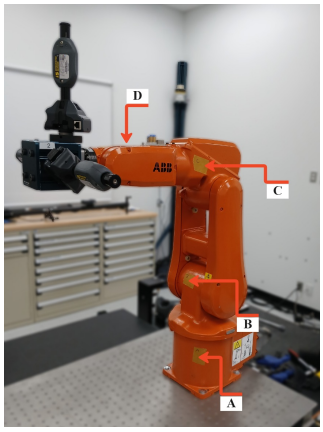

Figure. 4. Location of the gathered temperature measurements on the robot.

2) Transformation matrix between the iGPS frame and the robot base: To assess the resulting repeatability of the robotic arm with iGPS external encoders, the homogeneous transformation matrix between the iGPS reference frame and the robot base coordinate system must be determined. To achieve this, 5 data points were collected (1 cycle of the ISO 9283 cube from Fig. 1). The points used describe a 100 mm cube in the center of the robot workspace to limit the effects of flexion on the results. Also, a two-second average was used to collect coordinates from the iGPS receivers to reduce noise. Statistical analysis was then performed to identify the homogeneous transformation matrix. The transformation chain of the experimental setup is illustrated in Fig. 5. $\{iGPS\}$ is the coordinate system defined for the iGPS measurement system, $\{Base\}$ is the reference frame at the base of the robot, $\{Flange\}$ is the reference frame at the robot flange attachment point, and $\{Artifact\}$ is the reference frame constructed with the coordinates of 3 i5IS receivers placed on the artifact. T_1 to T_5 represent the homogeneous transformation matrices between the indicated frames. T_1 is constructed mathematically with the coordinates of the points provided by the i5IS receivers attached to the artifact. T_2 was constructed by measurements from a CMM. T_3 is determined by the inverse kinematics of the IRB120's controller, and T_4 is the unknown. T_4 can be determined for all data points collected with (7).

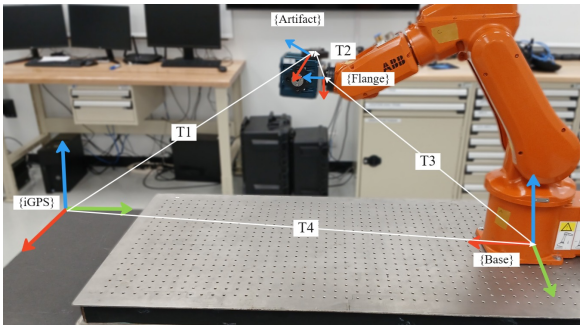

Figure. 5. Transformation matrix chain of the experimental setup.

$$T_4 = (T_3 T_2 T_1^{-1})^{-1} \tag{7}$$

3) Static Mounting Repeatability: The robot was consecutively moved to the five points defined by the ISO 9283 cube for 30 cycles. This time, the coordinates of the points were defined in the iGPS reference frame and translated into the robot base coordinate system using the established transformation matrix. This method simulates the positioning of a part within the environment. The iGPS coordinates were recorded for each point with a 2-second average, and the resulting repeatability was evaluated from the data. The direct measurement of positional and orientational repeatability of the $\{Artifact\}$ reference frame can be used to determine the positional and orientational repeatability of the key surface, since only one invariant transformation matrix separates them. This relationship is illustrated in Fig. 6, where $\{Key\}$ represents the key features' reference frame.

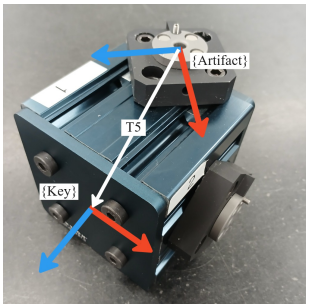

Figure. 6. Transformation matrix relationship between the artifact's frame of reference and a key feature of the simulated part

4) Detachment and Remounting Repeatability: The same test as the static mounting repeatability test was conducted, but this time the artifact was detached from the robot between each measurement. This approach further simulates a real assembly process. However, only 50 data points were collected (10 cycles of the ISO 9283 cube).

IV. Results

A. Ideal Warm-Up Time

The ideal warm-up time was determined to be 130 minutes for a low-speed movement in our test conditions, as shown in Fig. 7. The time to reach thermal stability is dependent on the robot's movement, the load, and the environmental conditions. For every subsequent test, a warm-up cycle of 130 minutes was used to mitigate thermal expansion effects on results.

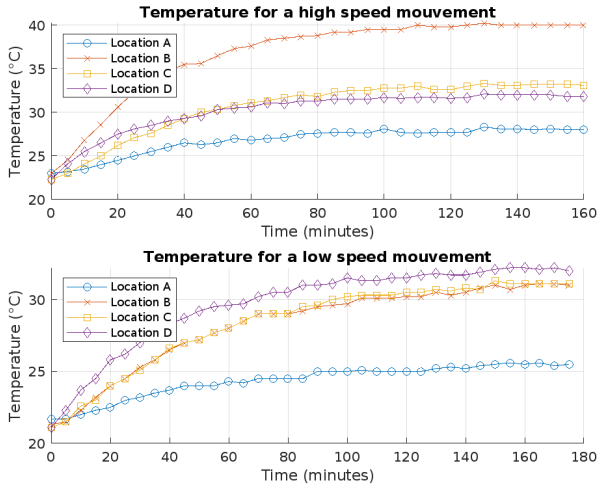

Figure. 7. Thermal stability test for a high speed movement and a low speed movement in similar tests conditions

B. Robot Base Positioning in the iGPS Reference Frame

For each of the 5 robot target positions, the coordinates of the three iGPS receivers on the artifact were recorded, and using (7), the resulting transformation matrix from $\{iGPS\}$ to $\{Base\}$ was computed, as shown in Fig. 5. Table I shows statistics on the resulting transformation matrix for the static mounting repeatability, while Table II shows the results of the same process for the detachment and remounting repeatability test. In both cases, no outlier datat points were obeserved.

TABLE. I
GATHERED DATA STATISTICS TO DETERMINE THE IDEAL TRANSFORMATION MATRIX BETWEEN $\{iGPS\}$ REFERENCE FRAME AND $\{Base\}$ REFERENCE FRAME FOR THE STATIC REPEATABILITY TEST

Value	Min	Max	Median	Mean	Std
X (mm)	317.43	319.66	318.35	318.52	0.82
Y (mm)	1382.84	1383.01	1382.87	1382.92	0.08
Z (mm)	52.71	54.30	53.32	53.47	0.71
Roll (deg.)	-89.46	-89.40	-89.42	-89.42	0.02
Pitch (deg.)	0.21	0.27	0.24	0.24	0.02
Yaw (deg.)	0.62	0.77	0.67	0.69	0.06

For better visualization, the translations along each axis and the roll (α), pitch (β), and yaw (γ) angles were extracted for every transformation matrix. The median was the chosen metric for reconstructing the ideal homogeneous transformation matrix. The larger standard deviation seen for the X translation and Z translation in Tables I and II is expected, considering the X and Z directions are most affected by flexion of the robot arm, thus resulting in inaccuracies. It is important to note that the high precision of this matrix is not a requirement for this study, since only the system's repeatability is evaluated.

TABLE. II
GATHERED DATA STATISTICS TO DETERMINE THE IDEAL TRANSFORMATION MATRIX BETWEEN $\{iGPS\}$ REFERENCE FRAME AND $\{Base\}$ REFERENCE FRAME FOR THE DETACHMENT REPEATABILITY TEST

Value	Min	Max	Median	Mean	Std
X (mm)	317.48	319.52	318.60	318.57	0.78
Y (mm)	1382.71	1383.15	1382.84	1382.91	0.17
Z (mm)	52.77	54.18	53.35	53.51	0.63
Roll (deg.)	-89.43	-89.39	-89.41	-89.41	0.01
Pitch (deg.)	0.22	0.26	0.24	0.24	0.02
Yaw (deg.)	0.64	0.76	0.68	0.69	0.05

However, if the same experimental setup is used to study the resulting precision, measures such as robot kinematic calibration and validation with more precise instruments may become necessary.

C. Static Mounting and Detachment Repeatability

The gathered data points were analysed to determine positional and orientation repeatability as defined by the ISO 9283 guidlines with equations (1) to (6) for points P1-P2-P3-P4-P5 of the cube. The mean repeatability for the static mounting test was observed to be approximately 31 μm while the detachment repeatability test yielded a mean repeatability across all tested positions of 26 μm. The results for both tests are presented in Table III and Table IV respectively. These results seem to indicate that the mechanical interface between the artifact and the robot's flange have negligible effect on the overall repeatability of the system. However, more data points are required to conclude this matter. Fig. 8 to Fig. 12 present the gathered data for both repeatability tests for positions P1 to P5. Only P1 showed a large difference between the the static repeatability test and the detachment repeatability as illustrated in Fig. 8. two data points in particular largely affect the overall repeatability. It is likely that the difference in reapatbility would be reduced if more data points are collected.

TABLE. III
POSE AND ORIENTATION REPEATABILITY EVALUATED FOR THE STATIC REPEATABILITY TEST WITH 150 DATA POINTS (30 CYCLES OF THE ISO 9283 CUBE)

Point	RP_l (mm)	RP_α (deg.)	RP_β (deg.)	RP_γ (deg.)
P1	0.0315	0.0221	0.0163	0.0281
P2	0.0325	0.0362	0.0090	0.0391
P3	0.0282	0.0261	0.0101	0.0314
P4	0.0281	0.0191	0.0156	0.0177
P5	0.0323	0.0219	0.0135	0.0248
Mean	0.0305	0.0251	0.0129	0.0282

V. CONCLUSIONS

These results validate the potential of a robot augmented with iGPS tracking as a robust system for guiding jigless assembly. The aim was to quantify the process repeatability capabilities. The mean positional repeatability, as defined by the ISO 9283 guidelines across the five measured positions, was 31 μm for static repeatability and 26 μm for the detachment repeatability test (both at 99.73% confidence). However, if more data is gathered, it is hypothesized that this difference would be reduced. The future research direction with the framework developed in this paper is twofold. First, it is necessary to go beyond the spherical approach to defining the uncertainty zone. An ellipsoid representation seems more appropriate for characterizing the repeatability error zone. Studying deviation distributions could further refine the repeatability model of the developed framework. Second, the robot's repeatability will be studied at the same five ISO cube points tested. This will contribute to the analysis by distinguishing the fraction of repeatability error attributable to the robot itself from the portion introduced by the iGPS measurement system.

TABLE. IV
POSE AND ORIENTATION REPEATABILITY EVALUATED FOR THE DETACHMENT REPEATABILITY TEST WITH 50 DATA POINTS (10 CYCLES OF THE ISO 9283 CUBE)

Point	RP_l (mm)	RP_α (deg.)	RP_β (deg.)	RP_γ (deg.)
P1	0.0406	0.0234	0.0260	0.0326
P2	0.0261	0.0142	0.0114	0.0246
P3	0.0253	0.0143	0.0081	0.0253
P4	0.0204	0.0276	0.0115	0.0245
P5	0.0175	0.0243	0.0098	0.0216
Mean	0.0260	0.0208	0.0134	0.0257

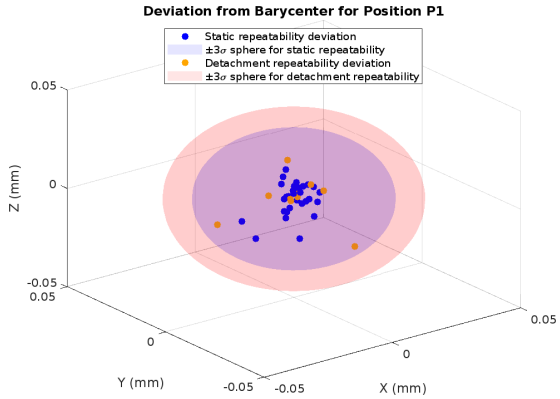

Figure. 8. Deviation from barycenter for position P1

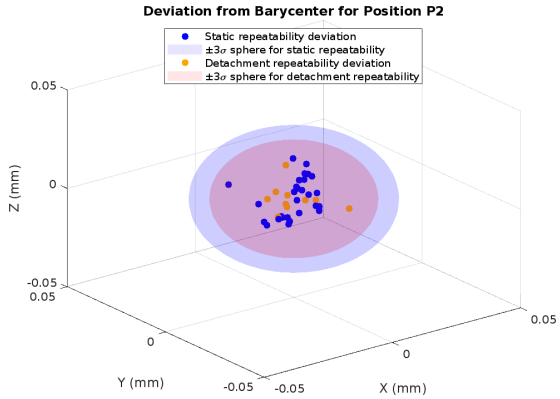

Figure. 9. Deviation from barycenter for position P2

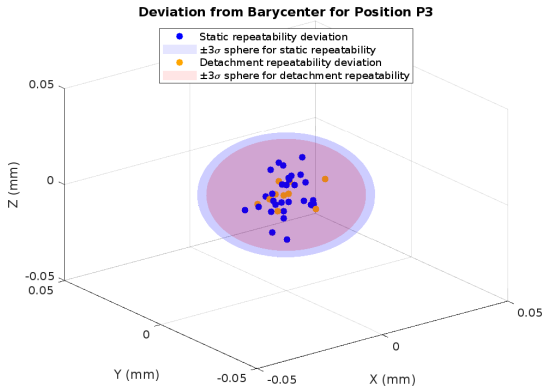

Figure. 10. Deviation from barycenter for position P3

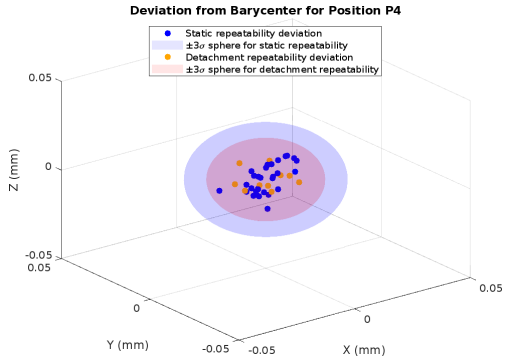

Figure. 11. Deviation from barycenter for position P4

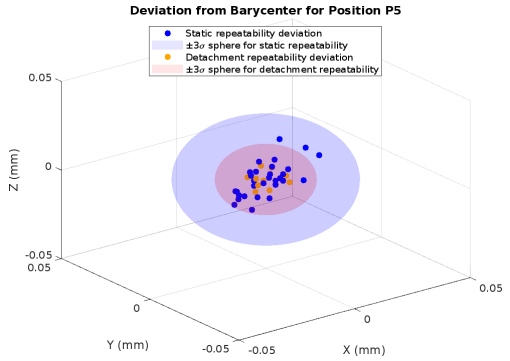

Figure. 12. Deviation from barycenter for position P5

REFERENCES

[1] J. E. Muelaner, Z. Wang, J. Jamshidi, *et al.*, "Study of the uncertainty of angle measurement for a rotary-laser automatic theodolite (r-LAT)," *Proceedings of the Institution of Mechanical Engineers, Part B: Journal of Engineering Manufacture*, vol. 223, no. 3, pp. 217–229, Mar. 1, 2009. DOI: 10.1243/09544054JEM1272.

[2] Z. Wang, L. Mastrogiacomo, F. Franceschini, and P. Maropoulos, "Experimental comparison of dynamic tracking performance of iGPS and laser tracker," *The International Journal of Advanced Manufacturing Technology*, vol. 56, no. 1, pp. 205–213, Sep. 2011. DOI: 10.1007/s00170-011-3166-0.

[3] F. Franceschini, M. Galetto, D. Maisano, L. Mastrogiacomo, and B. Pralio, "Indoor GPS (iGPS™)," in *Distributed Large-Scale Dimensional Metrology: New Insights*, London: Springer, 2011, pp. 23–35.

[4] M. H. Miah, D. S. Chand, and G. S. Malhi, "Indoor global positioning measurement system: Application in aircraft assembly technology," presented at the Advancements in Civil Engineering: COSMEC-2021, Mohali, India, 2023, p. 020015. DOI: 10.1063/5.0119959.

[5] A. R. Norman, A. Schönberg, I. A. Gorlach, and R. Schmitt, "Validation of iGPS as an external measurement system for cooperative robot positioning," *The International Journal of Advanced Manufacturing Technology*, vol. 64, no. 1, pp. 427–446, Jan. 2013. DOI: 10.1007/s00170-012-4004-8.

[6] 7. K. Metrology. "6th generation technology further increases iGPS usability & performance." Accessed: December 12, 2024. (2024), [Online]. Available: https://7dkmetrology.com/7dk-1/i5is-en.

[7] R. Schmitt, W. Kimmelmann, S. Quinders, C. Storm, and F. Oberhansberg, "Investigation of the applicability of an iGPS metrology system to automate the assembly in motion of a truck cabin," *Applied Mechanics and Materials*, vol. 840, pp. 58–65, Jun. 2016. DOI: 10.4028/www.scientific.net/AMM.840.58.

[8] C. Storm, A. Schönberg, and R. H. Schmitt, "Model predictive control approach for assembling large components in motion," *Production Engineering*, vol. 11, no. 2, pp. 167–173, Apr. 2017. DOI: 10.1007/s11740-017-0717-8.

[9] R. Han, E. Trostmann, and T. Dunker, "Research on the method of improving iGPS dynamic tracking accuracy based on theoretical trajectory backward compensation," *Advances in Mechanical Engineering*, vol. 15, no. 5, p. 16878132231170771, May 2023. DOI: 10.1177/16878132231170771.

[10] F. Shi, N. Sun, Z. Du, and L. Liu, "Real-time measurement and compensation based on iGPS for industrial robotic pose accuracy," *Journal of Physics: Conference Series*, vol. 2591, Sep. 1, 2023. DOI: 10.1088/1742-6596/2591/1/012058.

[11] G. Heiden and M. D. C. Porath, "Metrological performance of indoor-GPS in a simulated measurement assisted assembly process," *Journal of Physics: Conference Series*, vol. 733, p. 012036, Jul. 2016. DOI: 10.1088/1742-6596/733/1/012036.

[12] M. Vocetka, Z. Bobovský, J. Babjak, *et al.*, "Influence of drift on robot repeatability and its compensation," *Applied Sciences*, vol. 11, no. 22, p. 10813, Nov. 16, 2021. DOI: 10.3390/app112210813.

[13] M. Slamani, A. Joubair, and I. A. Bonev, "A comparative evaluation of three industrial robots using three reference measuring techniques," *Industrial Robot: An International Journal*, vol. 42, no. 6, pp. 572–585, Oct. 19, 2015. DOI: 10.1108/IR-05-2015-0088.